Research Square

Preprints are preliminary reports that have not undergone peer review.
They should not be considered conclusive, used to inform clinical practice,
or referenced by the media as validated information.

Layer-specific effects of ultra-speed sintering on the translucency and microstructure of yttria-gradient zirconia

Hye-Jeong Shin
Pusan National University
Mi-Hyang Cho
Wonkwang University
Hyo-Joung Seol
seol222@pusan.ac.kr

Pusan National University

Article

Keywords: Translucency, Microstructure, Ultra-speed sintering, Yttria-gradient zirconia

Posted Date: September 1st, 2026

DOI: https://doi.org/10.21203/rs.3.rs-10662394/v1

License: This work is licensed under a Creative Commons Attribution 4.0 International License.
Read Full License

Additional Declarations: No competing interests reported.

Abstract

This study evaluated the effects of ultra-speed (US) sintering on the translucency and microstructure of yttria-gradient zirconia. Eighty specimens were prepared from two yttria-gradient zirconias (5 mol% yttria-stabilized incisal and 4 mol% yttria-stabilized cervical layers). Each layer underwent conventional (CS) or US sintering. Translucency (TP_{00}) was measured spectrophotometrically (n = 10/group). Microstructure, grain size, and phase composition were analyzed using field-emission scanning electron microscopy (n = 4/group) and Rietveld refinement (n = 2/group). Translucency was analyzed using three-way ANOVA, and grain size using a generalized linear model (α = 0.05). Under CS, the incisal layer (TP_{00}: 8.01–8.12) was more translucent than the cervical layer (7.27–7.45), whereas this relationship was reversed after US sintering. This reversal reflected a significant reduction in TP_{00} in the incisal layer (ΔTP_{00}: 2.78–3.00), exceeding the translucency acceptability threshold, while cervical changes remained within the translucency perceptibility threshold. Residual pores were more evident in the incisal layer after US sintering, with grain size increasing from 1.13–1.14 to 2.94–2.98 μm. After US sintering, the yttria-rich *t*′-phase fraction increased, whereas the *t*-phase fraction decreased in both layers. These findings provide further insight into the potential layer-specific response of yttria-gradient zirconias to US sintering.

Introduction

Zirconia has become a preferred restorative material owing to its excellent mechanical strength and esthetic properties. The advent of induction and electromagnetic heating furnaces has enabled ultra-speed (US) sintering of zirconia in under 20 min[1–4], a marked reduction compared to conventional (over 7 h) and speed (approximately 60–120 min) sintering protocols[1–7]. Previous studies have generally reported reduced translucency in 5 mol% yttria partially stabilized zirconia (5Y-PSZ) following US sintering, although stable translucency has also been reported in some studies[1–3,8,9]. Despite these previous findings, little is known about how US sintering affects the translucency and microstructural characteristics of recently developed yttria-gradient zirconias. Typically, yttria-gradient zirconias combine a high-strength, lower-yttria layer (cervical) composed of 3 mol% yttria-stabilized tetragonal zirconia polycrystals (3Y-TZP) or 4 mol% yttria partially stabilized zirconia (4Y-PSZ) with a high-translucency, higher-yttria layer (incisal) composed of 5Y-PSZ to achieve esthetics comparable to natural teeth[10–13]. However, at a given yttria content, the optical properties of zirconia are closely related to its microstructure[2]; thus, the intended optical performance of yttria-gradient zirconias may depend, in part, on the final microstructure developed during sintering[14].

As zirconia possesses a high refractive index, strong light scattering typically occurs at grain boundaries, internal pores and interfaces with other phases[15]. Among these, internal pores have been reported as a major factor affecting translucency owing to the high refractive index (n) mismatch between zirconia (n = 2.160) and air within pores (n = approximately 1)[15–20]; even an extremely low porosity of 0.01% can reduce translucency by up to 50%[17]. Because most commercially available dental zirconia materials are

supplied in a porous, pre-sintered state, achieving rapid densification and effective pore elimination is essential during US sintering to ensure translucency comparable to that achieved with conventional sintering (CS), as well as adequate mechanical strength[1–3,8,21].

The rapid heating rates of US sintering exacerbate the thermal gradient within zirconia because of its low thermal conductivity[22]. This temperature difference can trigger premature surface densification, obstructing diffusion paths and trapping internal pores, which may lead to insufficient sintering within the zirconia interior[8,9,22–24]. Furthermore, a higher yttria content in zirconia can accelerate grain growth during sintering[21,25], potentially allowing grain boundary migration to outpace pore elimination and thereby promoting pore entrapment within the grains[21]. Consistent with these mechanisms, previous studies have reported that 5Y-PSZ appears to be particularly susceptible to US sintering, exhibiting residual pore formation, increased grain size, and reduced translucency[2,9].

The rapid cooling rates inherent in US sintering protocols can also influence the phase transformations in zirconia by promoting the formation of an yttria-rich tetragonal phase (*t*′-phase)[26,27]. The *t*′-phase exhibits reduced tetragonality compared with the typical yttria-lean tetragonal phase (*t*-phase) because its axial ratio is closer to unity than that of the *t*-phase[26,27]. Consequently, the *t*′-phase and cubic phase have often been treated without clear distinction in previous studies because of their crystallographic similarity and overlapping diffraction patterns[27,28]. However, recent studies have indicated that 3–6 mol% yttria-stabilized zirconia consists of the *t*- and *t*′-phases rather than the *t*- and cubic phases previously assumed[28]. Accordingly, an increase in the *t*′-phase fraction can enhance translucency by reducing the light scattering caused by birefringence[5,27]. However, if residual pores are formed during US sintering, they may increase light scattering[9,17,29], potentially offsetting the optical benefits associated with the increased *t*′-phase fraction and thereby reducing translucency[9].

Given these factors, yttria-gradient zirconia may exhibit a layer-specific response to US sintering because of its heterogeneous yttria distribution, unlike zirconia with a uniform yttria distribution. However, the layer-specific effects of US sintering on the translucency, microstructure, and phase distribution of yttria-gradient zirconia have rarely been explored. Therefore, this study aimed to evaluate the impact of US sintering on the layer-specific translucency, microstructure, and phase distribution of yttria-gradient zirconias (5Y-PSZ/4Y-PSZ) compared with CS. The null hypothesis was that the sintering protocol would not significantly affect the translucency, microstructure, or phase distribution of either the incisal or cervical layer.

Methods

Sample preparation

This in vitro study employed a 2 × 2 × 2 factorial design, incorporating 3 independent variables: 2 zirconia materials, 2 layers (incisal and cervical), and 2 sintering protocols (CS and US). The sample size was

determined by a power analysis using G*Power software (version 3.1.9.7; Heinrich Heine University Düsseldorf, Düsseldorf, Germany)[1]. To detect a significant difference with a large effect size (f = 0.40) and an α level of 0.05, a total sample size of 80 specimens (n = 10/group) was required to achieve a statistical power of 0.94.

Specimens were prepared from A2-shaded, yttria-gradient zirconia materials, with the compositions and layer specifications summarized in Table 1: IPS e.max ZirCAD Prime Esthetic (EST) and IPS e.max ZirCAD MT Multi (MT) (Ivoclar Vivadent, Schaan, Liechtenstein). According to the layer ratios or thicknesses specified by the manufacturer, the incisal (5Y-PSZ) and cervical (4Y-PSZ) layers were separated from the top and bottom sections of each material, respectively, using a diamond cutter (AMC-200, Fairworks, Seoul, Republic of Korea). Subsequently, both surfaces were dry-polished with SiC abrasive paper (800 to 5000 grit) to a presintered thickness of 1.25 mm, accounting for the approximately 20% linear sintering shrinkage, with the dimensions verified using a digital micrometer. For the US protocol, an 18-min cycle (Table 2) was selected from the pre-installed programs of a dedicated furnace (Programat SpeedFire, Dentsply Sirona, Charlotte, NC, USA). Conventional sintering (CS; control group) was performed for approximately 9.5 h (Table 2) using a separate furnace (InLab Profire, Dentsply Sirona, Charlotte, NC, USA). The final specimen dimensions after sintering were approximately 9 × 9 mm (width and length), with a thickness of 1.03 ± 0.01 mm. Representative sintered specimens and the US sintering profile are shown in Fig. 1.

Table 1
Chemical compositions and layer specifications of the yttria-gradient zirconia materials as supplied by the manufacturer

Material	**Layer ratio/thickness**	**Chemical composition (wt%)**				
		ZrO_2	**HfO_2**	**Y_2O_3**	**Al_2O_3**	**Others**
MT (IPS e.max ZirCAD MT Multi)	Top 20%: Incisal zone (5Y-PSZ) Middle 20%: Transition zone Bottom 60%: Cervical zone (4Y-PSZ)	86.0 – 93.5	≤ 5.0	6.5–8.0	≤ 1.0	≤ 1.0
EST (IPS e.max ZirCAD Prime Esthetic)	Top 3 mm: Incisal zone (5Y-PSZ) Middle 4 mm: Transition zone Bottom 7–18 mm: Cervical zone (4Y-PSZ)	86.0 – 93.5	≤ 5.0	6.5–8.3	≤ 1.0	≤ 1.0

Table 2
Detailed parameters of the used sintering protocols

Protocol	Stage	Heating and Cooling rate (°C/min)	Temp. (°C)	Holding time (min)
CS (total ~ 9.5 h)	Heating	10	900	30
	Sintering	3	1500	120
	Initial cooling	-10	900	0
	Final cooling and door open	-8	300	0
US (total ~ 18 min)	Heating	≈ 332	1000	0
	Sintering 1	≈ 111	1500	0
	Sintering 2	≈ 30	1580	4.48
	Cooling and door open	≈ -145	1110	0

CS, conventional sintering; US, ultra-speed sintering. The parameters for the US protocol were derived from direct measurements of the time elapsed during the sintering cycles.

Translucency measurement

The translucency was evaluated (n = 10/group) using a spectrophotometer (CM-3600d, Konica Minolta Sensing, Osaka, Japan; D65, 2° observer) and software (SpectraMagic NX version 2.02, Konica Minolta Sensing, Osaka, Japan)[15,30]. The spectral reflectance (360 to 740 nm, 10 nm increments) was measured in triplicate against white (L^* = 96.51, a^* = -0.11, b^* = -0.17) and black (L^* = 4.66, a^* = 1.06, b^* = -0.67) backgrounds. Glycerin was used as the optical coupling medium. The values of the translucency parameter (TP_{00}) were determined by calculating the CIEDE2000 color difference (ΔE_{00}) between the white and black backgrounds. The computation used the following formula[6,31]:

CIEDE2000 (ΔE_{00}) = $\left[\left(\frac{\Delta L'}{K_L S_L}\right)^2 + \left(\frac{\Delta C'}{K_C S_C}\right)^2 + \left(\frac{\Delta H'}{K_H S_H}\right)^2 + R_T\left(\frac{\Delta C'}{K_C S_C}\right)\left(\frac{\Delta H'}{K_H S_H}\right)\right]^{1/2}$, where $\Delta L'$, $\Delta C'$, and $\Delta H'$ denote variations in the lightness, chroma, and hue, respectively. The parametric factors K_L, K_C, and K_H were set to unity[6,31]. Weighting functions (S_L, S_C, and S_H) and a rotation function (R_T) were incorporated to adjust for visual perceptibility[6,31]. The clinical significance was interpreted using the CIEDE2000 50:50% perceptibility and acceptability thresholds for translucency (TPT = 0.62 and TAT = 2.62, respectively)[32].

Microstructural analysis

For microstructural characterization, four specimens were randomly selected from each group. The specimens were thermally etched at 1400°C for 30 min with a heating rate of 25°C/min and then cooled naturally to reveal the grain boundaries[2]. Subsequently, the specimens were platinum-coated for 90 s and examined using field-emission scanning electron microscopy (FE-SEM; JSM-7200F, JEOL, Akishima, Japan) at an accelerating voltage of 15 kV.

The mean grain size (D) was determined using the linear intercept method with ImageJ software (National Institutes of Health, Bethesda, MD, USA) by analyzing at least 600 grains per group from the obtained FE-SEM images[3,21]. The mean grain size was calculated using the formula $D = 1.56C/(MN)$, where C, M, and N represent the test line length, magnification, and number of intercepts, respectively[21].

X-ray diffraction analysis

High-resolution X-ray diffraction analysis (X'Pert^3 Powder, PANalytical, Amsterdam, the Netherlands) was performed (n = 2/group) using Ni-filtered CuKα radiation (40 kV, 30 mA). Data were collected over a 2θ range of 25 to 90° with a step size of 0.013°. The phase fractions were determined by Rietveld refinement using TOPAS-Academic V 7.23 (Bruker AXS, Karlsruhe, Germany). The space groups used were $P4_2/nmc$ (tetragonal), $Fm3m$ (cubic), and $P2_1/c$ (monoclinic)[27]. Crystallographic information files provided by Lamas and Walsoede Reca[33] and Howard et al.[34] were sourced from the Crystallography Open Database. Refinement quality was confirmed by a weighted profile R-factor (R_{wp}) below 10%[27]. The yttria content in the tetragonal phase was calculated using an established conversion formula[6,9].

Statistical analysis

Data were analyzed using SPSS 25.0 (IBM Corp., Armonk, NY, USA) at a significance level of $\alpha = 0.05$. Normality was assessed using the Shapiro–Wilk test ($p > 0.05$), and homogeneity of variances was evaluated using Levene's test ($p > 0.05$). The translucency data were analyzed using three-way ANOVA followed by Bonferroni post-hoc comparisons and simple main effects analyses. For grain size data exhibiting heteroscedasticity, a generalized linear model with robust standard errors was employed, followed by Bonferroni-adjusted pairwise comparisons.

Results

The three-way ANOVA (Table 3) indicated that the interaction between the sintering protocol and layer (S · L) exhibited the strongest influence on translucency ($p < 0.001$, *partial* $\eta^2 = 0.910$), followed by the sintering protocol ($p < 0.001$, *partial* $\eta^2 = 0.870$).

Table 3
Results of three-way ANOVA for translucency parameter (TP_{00})

Source of variation	Type III Sum of Squares	*df*	Mean Square	*F*	*p*	*Partial* η^2
Corrected model	100.318[a]	7	14.331	206.017	< 0.001	0.952
Intercept	3990.701	1	3990.701	57368.185	< 0.001	0.999
Zirconia material (Z)	0.247	1	0.247	3.556	0.063	0.047
Sintering protocol (S)	33.546	1	33.546	482.239	< 0.001	0.870
Layer (L)	15.577	1	15.577	223.933	< 0.001	0.757
Z × S	0.119	1	0.119	1.712	0.195	0.023
Z × L	0.248	1	0.248	3.567	0.063	0.047
S × L	50.559	1	50.559	726.806	< 0.001	0.910
Z × S × L	0.021	1	0.021	0.306	0.582	0.004
Error	5.009	72	0.070			
Total	4096.028	80				
Corrected total	105.327	79				

[a] *R* squared = 0.952 (Adjusted *R* squared = 0.948).

In the TP_{00} analysis (Table 4), the incisal layer exhibited higher TP_{00} values than the cervical layer under CS conditions in both materials ($p < 0.001$). However, this relationship was reversed under US conditions ($p < 0.001$). Specifically, compared with that under CS (TP_{00}: 8.01 to 8.12), TP_{00} in the incisal layer significantly decreased under US (ΔTP_{00}: 2.78 to 3.00, $p < 0.001$), exceeding the TAT (2.62)[32]. By contrast, compared with that under CS (TP_{00}: 7.27 to 7.45), TP_{00} in the cervical layer increased slightly under US (ΔTP_{00}: 0.25 to 0.34, $p < 0.01$), remaining well within the TPT (0.62)[32]. When the sintering protocol and layer were identical, no differences in TP_{00} were observed between the two zirconia materials ($p > 0.05$).

Table 4
Average translucency parameter (TP_{00}) values (mean ± SD) for each group of zirconia specimens

Layer	Material	CS	US	ΔTP_{00}	*p*-value (Effect of sintering protocol)
Incisal (5Y-PSZ)	**MT**	8.12 ^{B}	5.12 ^{A}	3.00	< 0.001
		(0.35)	(0.35)		
	EST	8.01 ^{B}	5.23 ^{A}	2.78	< 0.001
		(0.30)	(0.30)		
Cervical (4Y-PSZ)	**MT**	7.27 ^{A}	7.52 ^{B}	0.25	0.008
		(0.21)	(0.17)		
	EST	7.45 ^{A}	7.79 ^{B}	0.34	< 0.001
		(0.20)	(0.15)		

CS, conventional sintering; EST, Prime Esthetic; MT, MT Multi; US, ultra-speed sintering. ΔTP_{00} represents the absolute difference between CS and US. Same uppercase letters in a column indicate no statistically significant difference among groups ($p > 0.05$).

Microstructural analysis (Fig. 2a-d) revealed that the as-received microstructure of the two yttria-gradient zirconias consisted of aggregated nanoparticles in both layers. In the sintered state (Fig. 2e-l), compared with the CS groups (left), the US groups (right) exhibited residual pores both within grain interiors and at grain boundaries in the incisal layer (Fig. 2e-h) across both zirconia materials. In contrast, residual pores were less evident in the cervical layer (Fig. 2i-l) than in the incisal layer, although some residual pores were still observed after US sintering. Grain size analysis (Table 5) revealed that the grain size of the incisal layer increased from 1.13–1.14 μm under CS to 2.94–2.98 μm under US, regardless of the zirconia material ($p < 0.001$). In contrast, the cervical layer maintained a consistent grain size of 0.58–0.59 μm, regardless of the sintering protocol or the zirconia material ($p > 0.05$).

Table 5
Average grain size (mean ± SD, μm) for each group of zirconia specimens

Layer	Material	CS	US	*p*-value (Effect of sintering protocol)
Incisal (5Y-PSZ)	**MT**	1.14^{B}	2.98^{B}	< 0.001
		(0.13)	(0.36)	
	EST	1.13 ^{B}	2.94 ^{B}	< 0.001
		(0.16)	(0.32)	
Cervical (4Y-PSZ)	**MT**	0.59 ^{A}	0.58 ^{A}	0.503
		(0.06)	(0.06)	
	EST	0.58 ^{A}	0.59 ^{A}	0.135
		(0.04)	(0.04)	

CS, conventional sintering; EST, Prime Esthetic; MT, MT Multi; US, ultra-speed sintering. Same uppercase letters within a column indicate no statistically significant difference among groups ($p > 0.05$).

The Rietveld refinement results (Table 6) indicated that all specimens consisted of a mixture of yttria-lean *t*-phase and yttria-rich *t*′-phase, with the latter exhibiting an axial ratio closer to unity. In both materials, the incisal layer exhibited a higher *t*′-phase fraction than the cervical layer, and US sintering resulted in a substantial increase in the *t*′-phase fraction with a concomitant decrease in the *t*-phase fraction. Specifically, in the incisal layer, the *t*′-phase fraction rose from 62.55–63.89 wt% in the CS group to 80.22–81.50 wt% in the US group. A similar trend was observed in the cervical layer, where the *t*′-phase fraction increased from 40.26–42.10 wt% to 50.77–55.66 wt% following US sintering.

Table 6
Phase fractions (wt%), yttria content, and axial ratios ($c/a\sqrt{2}$) of each phase determined by Rietveld refinement for the zirconia specimens (mean ± SD).

Layer	Material	Parameter	CS		US	
			t-phase	*t'*-phase	*t*-phase	*t'*-phase
Incisal (5Y-PSZ)	**MT**	Fraction (wt%)	36.11 (2.11)	63.89 (2.11)	19.78 (1.79)	80.22 (1.79)
		Yttria content	3.17 (0.04)	7.37 (0.07)	3.55 (0.03)	6.22 (0.03)
		Axial ratio ($c/a\sqrt{2}$)	1.0142 (0.0004)	1.0042 (0.0002)	1.0133 (0.0001)	1.0069 (0.0001)
	EST	Fraction (wt%)	37.45 (1.17)	62.55 (1.17)	18.50 (1.18)	81.50 (1.18)
		Yttria content	3.15 (0.19)	7.32 (0.01)	3.38 (0.07)	6.17 (0.02)
		Axial ratio ($c/a\sqrt{2}$)	1.0142 (0.0005)	1.0043 (0.0001)	1.0137 (0.0002)	1.0070 (0.0001)
Cervical (4Y-PSZ)	**MT**	Fraction (wt%)	59.74 (1.41)	40.26 (1.41)	49.23 (2.84)	50.77 (2.84)
		Yttria content	2.82 (0.02)	7.22 (0.48)	3.48 (0.25)	6.24 (0.03)
		Axial ratio ($c/a\sqrt{2}$)	1.0151 (0.0001)	1.0046 (0.0011)	1.0134 (0.0006)	1.0068 (0.0001)
	EST	Fraction (wt%)	57.90 (1.43)	42.10 (1.43)	44.34 (1.25)	55.66 (1.25)
		Yttria content	2.79 (0.03)	7.51 (0.41)	3.27 (0.43)	6.15 (0.20)
		Axial ratio ($c/a\sqrt{2}$)	1.0151 (0.0001)	1.0039 (0.0009)	1.0140 (0.0011)	1.0070 (0.0004)

CS, conventional sintering; EST, Prime Esthetic; MT, MT Multi; *t*-phase, yttria-lean tetragonal phase; *t'*-phase, yttria-rich tetragonal phase; US, ultra-speed sintering.

Discussion

This study demonstrated that US sintering resulted in a significant decrease in translucency compared with CS in the incisal layer (5Y-PSZ) of yttria-gradient zirconia, whereas the cervical layer (4Y-PSZ) remained relatively stable; therefore, the null hypothesis was rejected. The reduction in translucency in the incisal layer under US sintering exceeded the TAT ($\Delta TP_{00} > 2.62$)[32], suggesting that the resulting translucency difference may be clinically undesirable for anterior restorations. In contrast, the ΔTP_{00} values of the cervical layer remained within the TPT ($\Delta TP_{00} < 0.62$)[32], showing relative stability. These findings suggest a greater susceptibility of the higher-yttria layer to US sintering in the yttria-gradient zirconia evaluated. Furthermore, the incisal layer exhibited higher translucency than the cervical layer under CS conditions in both materials (Table 4), consistent with the intended esthetic design of yttria-gradient zirconia. However, this relationship was reversed after US sintering, with the cervical layer showing higher translucency than the incisal layer in both materials. A similar trend was reported by Salah et al.[8], who found that, after US sintering, 3Y-TZP exhibited higher translucency than 5Y-PSZ, whereas 5Y-PSZ was more translucent than 3Y-TZP under CS. Because yttria-gradient zirconias are designed to mimic the optical characteristics of natural teeth[10–13], the reversal in translucency observed in the present study may compromise their intended optical gradient.

In the present study, the translucency parameter (*TP*) values were calculated using the CIEDE2000 (TP_{00}) formula, which better accounts for human visual perception[14]. However, for direct comparison with natural teeth and previous literature, TP_{ab} values under CS were also calculated from the same spectrophotometric measurements using the traditional CIELAB formula[8], yielding *TP* values of 10.57–10.69 for the incisal and 10.13–10.45 for the cervical layers. Although the reported *TP* values vary according to the zirconia product and shade, the results of the present study were consistent with the ranges reported in the literature[2,5,6,8,27]. Nevertheless, the TP_{ab} values obtained under CS in the present study remained considerably lower than the translucency reported for natural human teeth at a 1-mm thickness (incisal: 18.7; cervical: 16.4)[10]. Thus, the significant decrease in translucency observed in the incisal layer under US sintering may further widen the esthetic gap between zirconia and natural teeth.

The microstructural analyses suggested that the marked reduction in translucency in the incisal layer after US sintering may be associated with increased light scattering from residual pores, which were more frequently observed in the incisal layer than in the cervical layer[2,9,18,20]. The microstructure in the as-received state consisted of uniformly distributed aggregates of nanoparticles with interparticle porosity. When high heating rates, such as those used in US protocols, are applied to such structures, densification can be hindered and the formation of large, trapped pores can be promoted[24]. In addition, the high heating rates used in US sintering are known to generate steep thermal gradients between the surface and the interior of zirconia, thereby promoting premature surface densification and restricting pore elimination[8,9,22–24]. This may partly explain why residual pores were observed in both layers after US sintering. However, the more frequent observation of residual pores in the 5Y-PSZ incisal layer suggests that the higher yttria content may have increased the susceptibility to pore retention during US sintering. Although multiple factors may be involved, this difference could be associated with a rapid

increase in grain size. Previous studies have shown that a higher yttria content in zirconia can enhance grain growth[21,25,35], potentially promoting pore entrapment during grain boundary migration[21]. The higher final temperature used in US protocols to compensate for the shortened sintering duration may further increase grain size[21,25,36]. Consequently, in zirconia with higher yttria contents, pores may be more likely to become trapped within enlarging grains before they can migrate to and escape through the grain boundaries[21]. These residual pores can act as light-scattering centers owing to the large refractive index mismatch between zirconia and the air within the pores[15–20]. This mechanism may at least partly explain why the 5Y-PSZ incisal layer was more susceptible to translucency loss under US sintering than the 4Y-PSZ cervical layer, with an apparent increase in grain size and more frequent residual pores observed in the incisal layer. Similar microstructural and optical changes have also been reported in 5Y-PSZ materials without a yttria-gradient design, with residual pores under US sintering accompanied by increased grain size and decreased translucency[2,9]. Although mechanical properties were not evaluated in the present study, residual pores have been associated with reduced flexural strength in 5Y-PSZ under US sintering[2,9].

The phase changes observed in the present study may also be related to the rapid cooling inherent in the US protocol[26,27]. A previous study showed that controlled rapid cooling after annealing at 1550°C for 1 h increased the yttria-rich *t*′-phase fraction by 5.3–11.6 wt%, with a concomitant decrease in the yttria-lean *t*-phase fraction in 3Y-TZP, 4Y-PSZ, and 5Y-PSZ[27]. Similarly, in the present study, the yttria-rich *t*′-phase fraction increased by 10.51–18.95 wt% across all layers under US sintering compared with CS, with a concomitant decrease in the yttria-lean *t*-phase fraction. Consistent with these findings, 5Y-PSZ subjected to US sintering has been reported to exhibit a 13 wt% increase in the *t*′-phase fraction (from 74 to 87 wt%)[9]. The reported axial ratio and yttria content of the *t*′-phase were also consistent with those observed in the present study[9]. The increase in the *t*′-phase fraction is generally associated with increased translucency because the *t*′-phase contains a higher yttria content and exhibits an axial ratio closer to unity than the optically anisotropic *t*-phase[27]. Consistent with this mechanism, in the cervical layer, an increase in the yttria-rich *t*′-phase fraction was accompanied by a slight increase in translucency under US sintering. In contrast, in the incisal layer, where residual pores were more evident than in the cervical layer, translucency significantly decreased compared with CS despite the increase in the *t*′-phase fraction. This suggests that the optical benefits associated with the increase in the *t*′-phase fraction[5,27] may have been outweighed by the light-scattering effects of the residual pores in the incisal layer[9,16–20]. This is consistent with previous findings showing that translucency decreased in 5Y-PSZ following US sintering despite an increased *t*′-phase fraction, while more residual pores were observed than under CS[9].

In the present study, no significant interaction was observed between the zirconia material and sintering protocol for translucency, suggesting that, for the two zirconia products evaluated, US sintering produced similar translucency responses. In both materials, US sintering reversed the intended translucency gradient, with the 4Y-PSZ layer exhibiting higher translucency than the 5Y-PSZ layer.

Microstructural changes were also similar in both materials, with increased grain size and more evident residual pores in the incisal layer under US sintering. However, this layer-specific response to US sintering may not be universal across all commercially available yttria-gradient zirconias. Previous studies evaluating yttria-gradient zirconias layer-by-layer under US sintering remain limited, making direct comparisons difficult. One such study evaluated the optical effects of US sintering on a yttria-gradient zirconia composed of 5Y-PSZ and 3Y-TZP[14]. In that study, unlike the present study, comparable reductions in translucency were observed in both the 5Y-PSZ incisal layer and the 3Y-TZP cervical layer following 15-min US sintering, without altering the intended translucency gradation from the cervical to the incisal layer[14]. However, direct comparison should be made with caution because different product formats intended for the respective sintering protocols were used for the US and CS groups in that study[14]. Nevertheless, color differences after US sintering were more pronounced in the 5Y-PSZ layer than in the 3Y-TZP layer, and the authors suggested that these differences may also be associated with residual pores[14]. Although color difference was not evaluated in the present study, this finding may suggest a greater optical sensitivity of the higher-yttria layer to US sintering. By contrast, a different translucency and microstructural responses have been reported for a 5Y-PSZ material without a yttria-gradient design following US sintering[1–3]. In those studies, grain size varied but remained below 2 μm, with no residual pores observed and translucency remaining stable[1–3]. These contrasting findings indicate that the translucency response to US sintering is likely influenced by multiple factors rather than by yttria content alone, including differences in compositional design, minor chemical additives, manufacturing processes, sintering protocols, and experimental methodologies[8,14,21,37]. Therefore, although the present findings may not apply uniformly across all products, they provide further insight into the potential layer-specific response of yttria-gradient zirconias to US sintering.

A limitation of this study is that the transition layer was excluded to minimize compositional overlap between adjacent layers and to enable independent evaluation of the incisal and cervical layers. In addition, residual porosity was assessed only qualitatively. Therefore, future studies incorporating the transition layer, as well as investigations using full-contour crown specimens together with quantitative porosity analysis or density measurements, are needed to further clarify the mechanism underlying the observed translucency reduction. Additional limitations of this study include the evaluation of a single US protocol and two commercial products, which may not represent all yttria-gradient zirconias. Furthermore, because this investigation focused primarily on the translucency of zirconia, further studies are needed to evaluate the effects of US sintering on other optical properties, as well as on mechanical properties such as flexural strength and fracture toughness.

Conclusions

US sintering of the evaluated yttria-gradient zirconias resulted in layer-specific changes in translucency and microstructure. The incisal layer (5Y-PSZ) exhibited a significant reduction in translucency, increased grain size, and more evident residual pores, whereas the cervical layer (4Y-PSZ) showed only minimal

changes in translucency with stable grain size. The yttria-rich *t*′-phase fraction increased in both layers following US sintering.

Declarations

Data availability

The datasets generated and/or analyzed during the current study are available from the corresponding author upon reasonable request.

Author contributions Hye-Jeong Shin: Methodology, Investigation, Formal analysis, Mi-Hyang Cho: Methodology, Investigation, Formal analysis. Hyo-Joung Seol: Conceptualization, Methodology, Investigation, Formal analysis, Writing—original draft, Writing—review & editing, Supervision.

References

1. Liu, H. et al. Influence of high-speed sintering protocol on translucency, mechanical properties, microstructure, crystallography, and low-temperature degradation of highly translucent zirconia. *Dent. Mater.* **38**, 451–468 (2022).
2. Lawson, N. C. & Maharishi, A. Strength and translucency of zirconia after high-speed sintering. *J. Esthet Restor. Dent.* **32**, 219–225 (2020).
3. Cokic, S. M. et al. Mechanical properties, aging stability, and translucency of speed-sintered zirconia for chairside restorations. *Dent. Mater.* **36**, 959–972 (2020).
4. Lee, S., Choi, G., Choi, J., Kim, Y. & Kim, H. K. Effect of high-speed sintering on the marginal and internal fit of CAD/CAM-fabricated monolithic zirconia crowns. *Sci. Rep.* **13**, 17215 (2023).
5. Shin, H. J., Kwon, Y. H. & Seol, H. J. Effect of superspeed sintering on translucency, opalescence, microstructure, and phase fraction of multilayered 4 mol% yttria-stabilized tetragonal zirconia polycrystal and 6 mol% yttria-stabilized partially stabilized zirconia ceramics. *J. Prosthet. Dent.* **130**, 254e1–e10 (2023).
6. Cho, M. H. & Seol, H. J. Impact of speed sintering on translucency, opalescence and microstructure of dental zirconia with a combination of 5 mol% and 3 mol% yttria-stabilized zirconia. *Materials* **17**, 5148 (2024).
7. Cho, M. H. & Seol, H. J. Effect of high-speed sintering on the optical properties, microstructure, and phase distribution of multilayered zirconia stabilized with 5 mol% yttria. *Materials* **16**, 5570 (2023).
8. Salah, K., Sherif, A. H., Mandour, M. H. & Nossair, S. A. Optical effect of rapid sintering protocol on different types of zirconia. *J. Prosthet. Dent.* **130**, 253e1–253e7 (2023).
9. Nonaka, K., Teramae, M. & Pezzotti, G. Evaluation of the effect of high-speed sintering and specimen thickness on the properties of 5 mol% yttria-stabilized dental zirconia sintered bodies. *Materials* **15**, 5685 (2022).

10. Lee, Y. K. Translucency of human teeth and dental restorative materials and its clinical relevance. *J. Biomed. Opt.* **20**, 045002 (2015).
11. Inokoshi, M. et al. Layer characteristics in strength-gradient multilayered yttria-stabilized zirconia. *Dent. Mater.* **39**, 430–441 (2023).
12. Biçer, E. Y., Öztürk, E. K. & Güngör, M. B. Strength-gradient multilayer zirconia ceramics: A narrative review of the mechanical and optical properties. *J. Am. Ceram. Soc.* **108**, e20711 (2025).
13. Özişçi, O. Optical gradient and translucency behavior of three multilayer monolithic zirconia systems: A spectrophotometric study. *Sci. Rep.* **16**, 19453 (2026).
14. Rahawi, O. S., Alkhalidi, E. F., Alsahafı, T. & Sulaiman, T. A. Optical properties of multi-yttria-layered zirconia: Influence of high-speed sintering protocol. *J. Esthet Restor. Dent.* 1–6. https://doi.org/10.1111/jerd.70186 (2026).
15. Shiraishi, T. & Watanabe, I. Thickness dependence of light transmittance, translucency and opalescence of a ceria-stabilized zirconia/alumina nanocomposite for dental applications. *Dent. Mater.* **32**, 660–667 (2016).
16. Zhang, F., Reveron, H., Spies, B. C., Van Meerbeek, B. & Chevalier, J. Trade-off between fracture resistance and translucency of zirconia and lithium-disilicate glass ceramics for monolithic restorations. *Acta Biomater.* **91**, 24–34 (2019).
17. Zhang, Y. Making yttria-stabilized tetragonal zirconia translucent. *Dent. Mater.* **30**, 1195–1203 (2014).
18. Juntavee, N. & Attashu, S. Effect of sintering process on color parameters of nano-sized yttria partially stabilized tetragonal monolithic zirconia. *J. Clin. Exp. Dent.* **10**, e794–e804 (2018).
19. Alves, M. F. R. P., Abreu, L. G., Klippel, G. G. P., Santos, C. & Strecker, K. Mechanical properties and translucency of a multi-layered zirconia with color gradient for dental applications. *Ceram. Int.* **47**, 301–309 (2021).
20. Shahmiri, R., Standard, O. C., Hart, J. N. & Sorrell, C. C. Optical properties of zirconia ceramics for esthetic dental restorations: A systematic review. *J. Prosthet. Dent.* **119**, 36–46 (2018).
21. Kim, B. K. et al. Mitigating grain growth in fully stabilized zirconia via a two-step sintering strategy for esthetic dental restorations. *Int. J. Appl. Ceram. Technol.* **20**, 856–868 (2023).
22. Chen, D. J. & Mayo, M. J. Rapid rate sintering of nanocrystalline ZrO_2-3 mol% Y_2O_3. *J. Am. Ceram. Soc.* **79**, 906–912 (1996).
23. Prajzler, V., Průša, S. & Maca, K. Rapid pressure-less sintering of fine grained zirconia ceramics: Explanation and elimination of a core-shell structure. *J. Eur. Ceram. Soc.* **39**, 5309–5319 (2019).
24. Chen, D. J. & Mayo, M. J. Densification and grain growth of ultrafine 3 mol% Y_2O_3-ZrO_2 ceramics. *Nanostruct. Mater.* **2**, 469–478 (1993).
25. Matsui, K., Yoshida, H. & Ikuhara, Y. Isothermal sintering effects on phase separation and grain growth in yttria-stabilized tetragonal zirconia polycrystal. *J. Am. Ceram. Soc.* **92**, 467–475 (2009).

26. Gibson, I. R. & Irvine, J. T. S. Qualitative X-ray diffraction analysis of metastable tetragonal (t') zirconia. *J. Am. Ceram. Soc.* **84**, 615–618 (2001).
27. Kim, H. K. Effect of a rapid-cooling protocol on the optical and mechanical properties of dental monolithic zirconia containing 3–5 mol% Y_2O_3. *Materials* **13**, 1923 (2020).
28. Nakamura, K. et al. Critical evaluations on the crystallographic properties of translucent dental zirconia ceramics stabilized with 3–6 mol% yttria. *Dent. Mater.* **40**, 1425–1451 (2024).
29. Ahmed, W. M., Troczynski, T., McCullagh, A. P., Wyatt, C. C. L. & Carvalho, R. M. The influence of altering sintering protocol on the optical and mechanical properties of zirconia: A review. *J. Esthet Restor. Dent.* **31**, 423–430 (2019).
30. Ebeid, K. et al. Effect of changes in sintering parameters on monolithic translucent zirconia. *Dent. Mater.* **30**, e419–e424 (2014).
31. Yılmaz Savaş, T. & Aykent, F. Effect of fabrication techniques on the optical properties of zirconia-based systems. *J. Prosthet. Dent.* **125**, 528e1–528e8 (2021).
32. Salas, M. et al. Translucency thresholds for dental materials. *Dent. Mater.* **34**, 1168–1174 (2018).
33. Lamas, D. G. & De Walsöe, N. E. X-ray diffraction study of compositionally homogeneous, nanocrystalline yttria-doped zirconia powders. *J. Mater. Sci.* **35**, 5563–5567 (2000).
34. Howard, C. J., Hill, R. J. & Reichert, B. E. Structures of the ZrO_2 polymorphs at room temperature by high-resolution neutron powder diffraction. *Acta Crystallogr. B Struct. Sci.* **44**, 116–120 (1988).
35. Sharif, A. A., Imamura, P. H., Mitchell, T. E. & Mecartney, M. L. Control of grain growth using intergranular silicate phases in cubic yttria stabilized zirconia. *Acta Mater.* **46**, 3863–3872 (1998).
36. Darmawan, B. A., Fisher, J. G., Trung, D. T., Sakthiabirami, K. & Park, S. W. Two-step sintering of partially stabilized zirconia for applications in ceramic crowns. *Materials* **13**, 1857 (2020).
37. Chin, C. H., Muchtar, A., Azhari, C. H., Razali, M. & Aboras, M. Influences of the processing method and sintering temperature on the translucency of polycrystalline yttria-stabilized tetragonal zirconia for dental applications. *Ceram. Int.* **44**, 18641–18649 (2018).

Figures

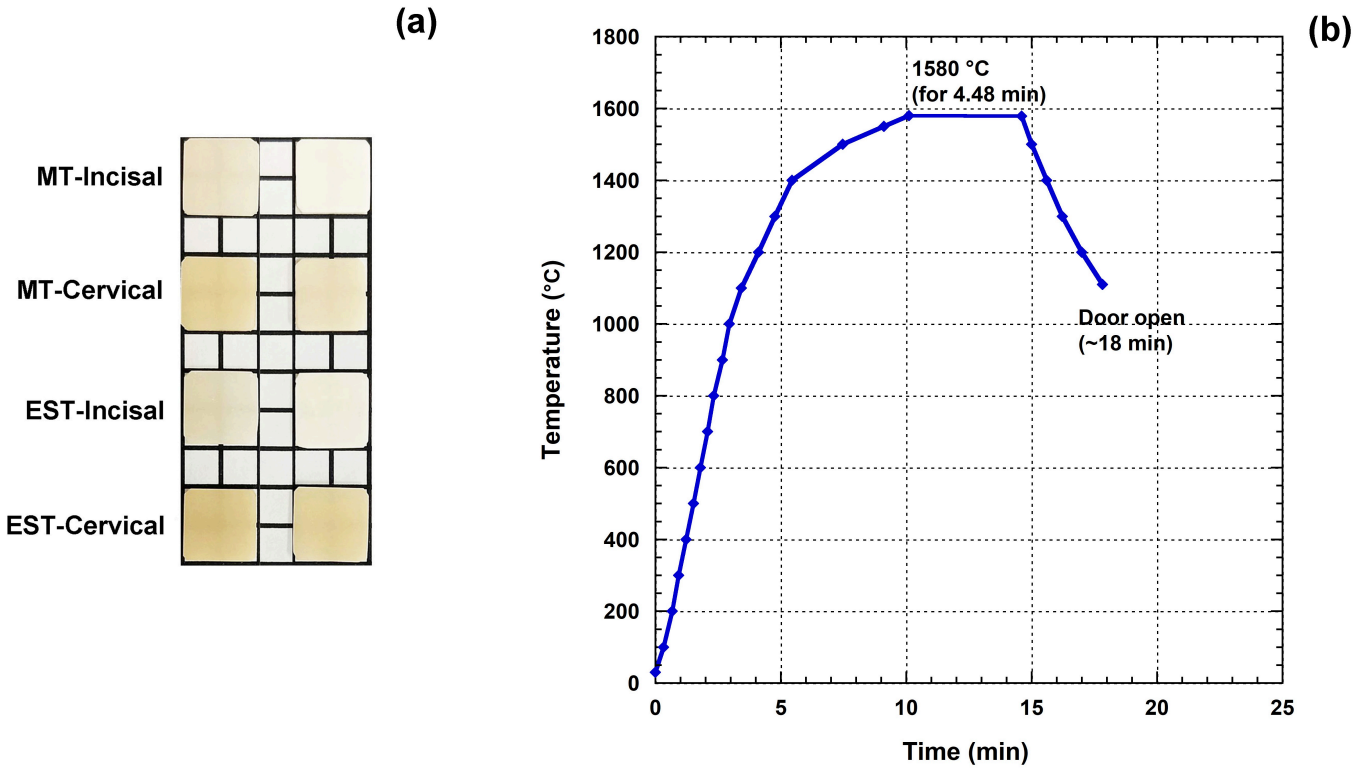


Figure 1

Sintered specimens and US sintering profile. (a) Representative sintered specimens from the incisal and cervical layers of MT and EST. Left and right columns represent CS and US sintering, respectively. (b) Temperature–time profile of the US sintering protocol. CS, conventional sintering; EST, Prime Esthetic; MT, MT Multi; US, ultra-speed sintering.

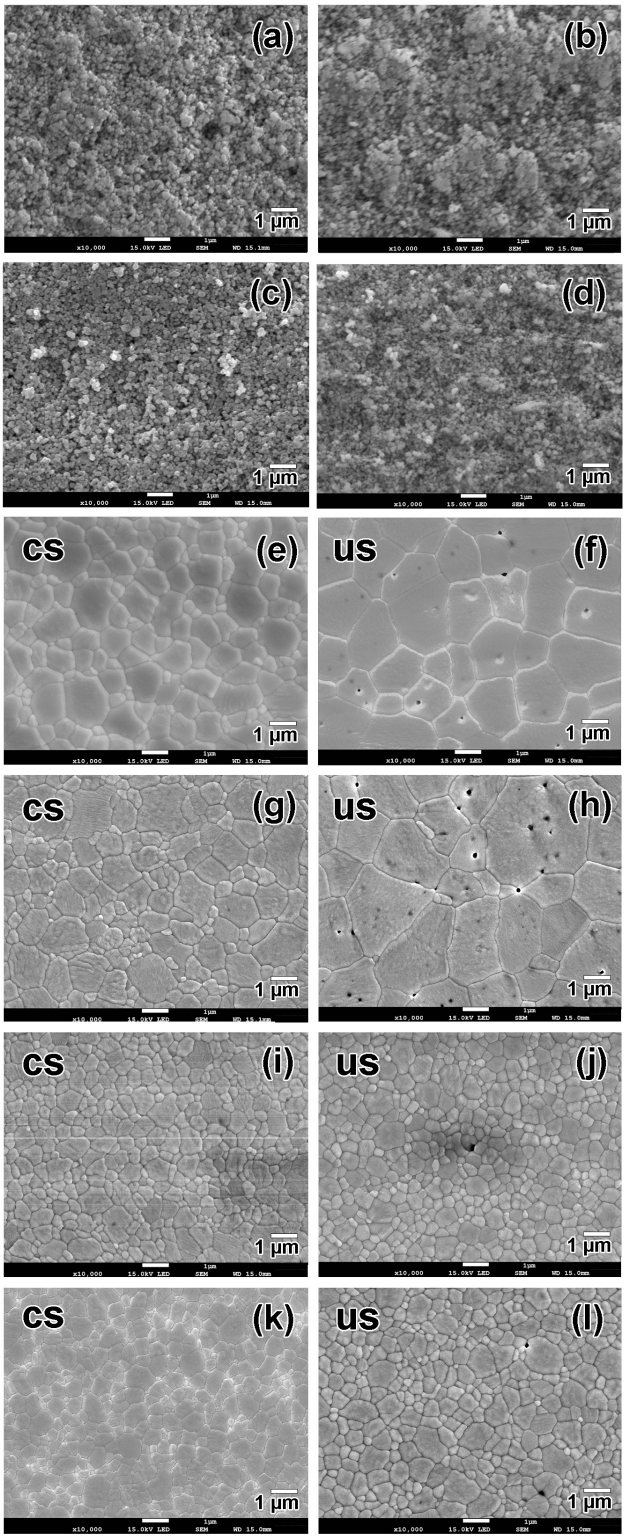


Figure 2

FE-SEM images of zirconia specimens in the as-received state and after CS and US sintering (original magnification ×10,000). (a, b) Incisal and cervical layers, respectively, of as-received MT; (c, d) Incisal and cervical layers, respectively, of as-received EST; (e, f) incisal layer of MT; (g, h) incisal layer of EST; (i, j) cervical layer of MT; and (k,l) cervical layer of EST. CS, conventional sintering; EST, Prime Esthetic; MT, MT Multi; US, ultra-speed sintering.